Version of Record: https://www.sciencedirect.com/science/article/pii/S1359645422009909
Manuscript_7a5d16f9e729e203d7e7d50237ea519a

Ferroelectric domain percolation in polycrystals

Sukriti Mantri[1], *John Daniels*[1]
[1]*Department of Materials Science and Engineering, UNSW Sydney, Kensington, Sydney, Australia, 2052*

Keywords

Multiferroics, domain percolation, domain continuity, ferroelectrics, grain boundary character, Crystallographic texture, ferroic polycrystals

Abstract

Ferroelectric materials possess the ability to switch between polarization states on application of external fields. This switching is facilitated via movement of domains walls and is a critical factor in the performance metrics of these materials. Hence, the interaction of domain walls with microstructural features such as grain boundaries can influence their performance. Experimentally, domain continuity has only been observed over a few grains with no information of the domain percolation length in larger polycrystals. For domain continuity to be energetically feasible, conditions of ferroelectric polarization continuity and domain wall plane matching need to be satisfied at the grain boundary. In this work, we have studied the extent of continuity of domains within modelled polycrystals. It is shown that under tighter conditions of plane matching and uncompensated polarization charge, favorable grain boundary character can have considerable impact on the domain percolation. However, when the conditions of domain continuity are relaxed, due to higher charge and geometric tolerance, domain percolation throughout the polycrystal is a likely phenomenon. It is shown that percolation of domains through a polycrystalline ferroelectric could be tailored by microstructural control of the grain boundary types and defect chemistry control of the charge compensation mechanisms. The ability to manipulate the length-scale of correlated domain wall motion may lead to new opportunities in ferroelectric functional device design. Additionally, these results can be extended to study the effect of grain boundary character on other material phenomena that involve planar interactions at grain boundaries, including ferroelastic twin boundaries and slip plane continuity.

Introduction

Ferroelectrics belong to a broader group of technologically important multiferroic materials that are utilized for their ability to have more than one spontaneous orientation states (polarization, magnetic spin, and/or strain) and switch between them on application of external stimuli (electric field, magnetic field and/or stress). Materials that are ferroelectric at lower temperatures, are in most cases, paraelectric (no spontaneous polarization) at high temperatures. The system develops polarization due to non-centrosymmetric nature of charge centers at the unit cell that develop at a transition temperature, also known as the Curie point. As the spontaneous polarization develops, depolarization energy also increases. To compensate for the depolarization energy, different regions of the crystal take different orientations of the spontaneous polarization [1,2]. These regions of uniform polarization are called domains and are separated by a domain wall. Domain walls fall on specific crystallographic planes, the orientation of which is decided by the polarization and strain tensor of the neighboring domains [3,4]. The walls are typically characterized as being a few unit cells thick for ferroelectrics, however more recent measurements in bulk polycrystals demonstrate strain fields covering several micrometers from the domain walls [5]. Domain walls are named according to the orientation difference between the polarization of neighboring domains. More broadly, 180° walls have opposite polarization states but equivalent spontaneous strain states, while non-180° walls have both different polarization and spontaneous strain states.

To reduce domain wall energy, permissible domain walls are ones that fulfill polarization continuity (i.e., the component of polarization vector along the normal to the domain wall is continuous across the domain wall) and strain compatibility (i.e., the strain mismatch on the domain wall is zero [3,4]). The domain walls are charge neutral in most cases. However, it should be noted that charged domain walls (CDWs) can exist and have been an area of recent interest[6]. The competition between different energies lead to different 3-dimensional arrangement/ordering of domains in a crystal also known as the domain structure. Common domain structures are alternating stripe domains, herring bone, square-net or watermark domains[7–10].

Domain switching is facilitated by the movement of domain walls. Reversible and non-reversible motion of domain walls contribute to the extrinsic dielectric and piezoelectric response of ferroelectrics [11–13]. Hence, mobility of domain walls is crucial to the response of ferroelectrics. This domain wall motion is clamped or pinned by defects [14–16] (dopants, vacancies, dislocations). In polycrystals, grain boundaries add an additional parameter that interferes with the mobility of domain walls. Grain boundary is a 2-dimensional defect that separate grains (regions of differently oriented unit cells) in polycrystals. Grain boundaries are also a sink for electronic and ionic defects creating space charge [17] which can also contribute to the pinning of domain walls at the grain boundaries. In order to ensure better performance in relatively more economic ferroelectric polycrystals, behavior of domains and domain walls around grain boundaries need to be better understood.

Ferroic domain structures have been observed to traverse grain boundaries in ferroelectrics. These continuous domains have been observed since the 1950s in $PbZr_xTi_{1-x}O_3$[18]and $BaTiO_3$[9,19–21]. Figure 1 shows microstructure images from select references demonstrating this domain continuity. In these cases, domain continuity through the grain boundaries is occurring, however it is limited around grain junctions and some regions of the grain boundaries. It can be seen in Figure 1 that continuity of the full domain pattern is not experimentally observed and in fact some domains do terminate at the grain boundary while others propagate. Unfortunately, observations of larger correlated domain structures in three dimensions are not currently available.

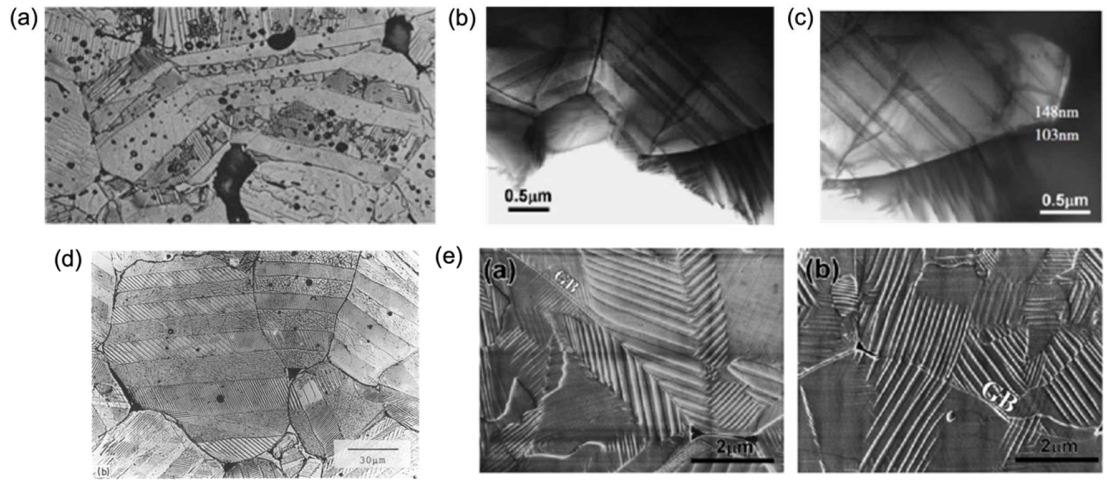

Figure 1: Micrographs showing continuous domains through grain boundaries for the following materials: (a) $BaTiO_3$ [9] *(published with permission from Elsevier), (b) $BaTiO_3$* [19] *(Copyright, 2007, The Japan Society of Applied Physics),(c) $BaTiO_3$* [22] *(Copyright, 2008, The Japan Society of Applied Physics),(d) $BaTiO_3$* [10]*(published with permission from AIP Publishing)(e) $PbZr_xTi_{1-x}O_3$* [18] *(published with permission from Elsevier)*

Continuous domains over grain boundaries can be argued to have a contribution on collective response of grains. Stimulus applied on one grain has been shown to impact the response of the neighboring grain possibly via the movement of these continuous domain structures [23]. The impact of grain boundaries on mobility of domains that traverse them is not clear, with some works arguing that they inhibit domain wall motion [10,24] while others suggest an increase in mobility [19,25].

Takahashi et. al. while relating domain size to piezoelectric properties in a polycrystalline $BaTiO_3$ sample also connected the higher d_{33} to continuous domains at grain boundaries [19]. With respect to understanding the geometrical conditions behind domain continuity, Tsurekawa et. al. [18] used coincidence site lattices and plane matching domains to support the evidence of continuous domains in $PbZr_xTi_{1-x}O_3$ wherein they concluded that the presence of grain boundaries that permitted plane matching with a twist deviation angle less than 20° were responsible for the observation of domain continuity. Recently, Mantri et. al. [26] developed the conditions required for domain continuity through any arbitrary grain boundary and then applied it to tetragonal, rhombohedral, and orthorhombic symmetries [27]. It was shown that these conditions and therefore domain continuity was a function of the five dimensions that define a grain boundary i.e., the three dimensions for the misorientation of the neighboring grains and two dimensions for the grain boundary plane normal. A very recent study of domain continuity in barium titanate [21] in which several bi-grains and tri-grain junctions were studied for domain continuity, found that domain continuity was possible even for large misorientations, finally concluding that domain continuity is possible for any misorientation as long as the compatibility for strain and charge are compensated. In the current study, geometrical plane matching(Equation 1) and grain boundary polarization charge (Equation 2) are the two conditions employed to study the probability of ferroic domain continuity. For further information on these two conditions, refer Mantri et. al. [26].

Although control of ferroic domain percolation holds unknown potential, the amount of investigation into the continuity of domains in ferroic microstructures, experimental as well as computational, has been minimal. Previous observations of domain wall continuity have only been made for a few grains, limiting any understanding of the length-scales over which they can propagate. In this work, the possibility for domains to percolate through model polycrystalline microstructures is investigated. We have calculated the domain percolation spread i.e.., the number of grain boundaries domains can continue through in a particular polycrystal. To relate domain percolation to processing variables, we have studied the effect of texturing and preferred grain boundary populations on domain percolation length. Crystallographic texturing has been shown to enhance piezoelectric response [28–30] in ferroelectrics, while $\sum 3$ type grain boundaries have been found to be highly favored in perovskites [31,32]. Investigating both of these cases, the magnitude of domain percolation is shown to increase. It is demonstrated that microstructural control can be used to vary the domain percolation behavior and thus may have a potentially significant influence over the degree of domain wall motion observed in these systems under external stimulus.

Methods

5-Dimensions of a grain boundary

A grain boundary is a 2-dimensional defect separating grains with different orientations. The grain boundary plane is defined by its normal which can be represented using two angles $\{\psi_1, \psi_2\}$ in the spherical orientation space. The crystallographic misorientation between the grains can be represented by three angles $\{\phi_1, \varphi, \phi_2\}$ that when applied successively changes the orientation of one grain to the another. Therefore, a grain boundary is represented using 5 dimensions: three dimensions for the grain-grain crystallographic misorientation and two dimensions for the grain boundary plane.

Mantri et. al. [26] describes in detail the conditions required for domain wall continuity at arbitrary grain boundaries. The two primary conditions are described in the following text.

Geometrical Plane Matching

For domains to be continuous over grain boundaries, domain walls need to geometrically match at the grain boundary. This condition is the geometrical plane matching condition (Figure 2). For two domain wall planes from neighboring grains to meet at the grain boundary, the angle of mismatch between the line of intersection of the domain walls in either grain with the grain boundary should be as small as possible, as represented by Equation 1. A geometric mismatch angle of zero would represent a perfect plane matching condition (Figure 2a). Any change in the orientation of domain walls that can happen on changing grain orientation and/or any change in the orientation of grain boundary plane would affect the geometrical plane

matching (Figure 2b-c). In this work, a tolerance angle was chosen which would be the maximum mismatch angle up to which successful geometric matching can be assumed to happen.

$$Geometrical\ mismatch\ angle = \cos^{-1}\{\hat{n}_{Grain\ Boundary\ Plane} \cdot (\hat{n}_{Domain\ wall\ in\ grain\ A} \times \hat{n}_{Domain\ Wall\ in\ grain\ B})\} \quad (1)$$

Grain Boundary Polarization Charge Continuity

As ferroelectric domains are uniform regions of polarization, for domain walls to continue over grain boundary, the polarization vector of the domains in neighboring grains should be continuous (Figure 3). This means that the difference in the component of polarization vectors of both the domains along the normal to the grain boundary plane should be as small as possible. This condition has been called grain boundary polarization charge continuity. It is represented by Equation 2. Similar to the geometric tolerance, a charge tolerance has been defined here as well. Below this tolerance it is assumed the charge mismatch can be accommodated by other mechanisms at the grain boundary.

$$Residual\ Grain\ Boundary\ Polarization\ Charge = \{(\hat{n}_{Grain\ Boundary\ Plane} \cdot \hat{P}_{Polarization\ in\ grain\ A}) - (\hat{n}_{Grain\ Boundary\ Plane} \cdot \hat{P}_{Polarization\ in\ grain\ B})\} \quad (2)$$

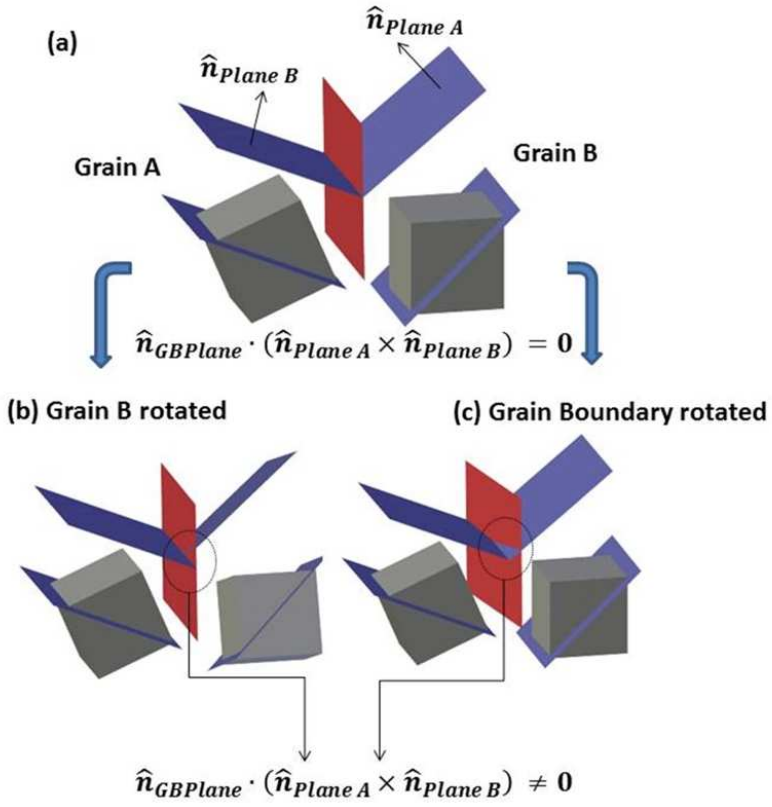

Figure 2: The condition of geometrical plane matching of a domain wall plane (blue planes) at a grain boundary (red plane). (a) a perfect geometrically matched arrangement. (b) shows geometrical mismatch due to change in grain-grain misorientation. (c) shows geometrical mismatch due to change in grain boundary plane orientation. Image reprinted from Acta Materialia, 128, Mantri et. al., Ferroelectric Domain Continuity over grain boundaries, 400-405, 2017, with permission from Elsevier [26].

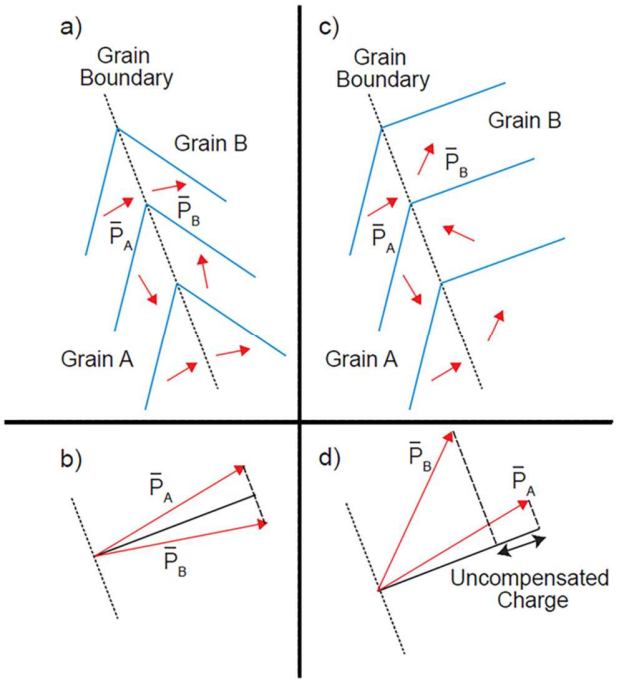

Figure 3: The condition of polarization charge continuity at a grain boundary (dashed line). (a) shows the perfect polarization continuity where the component of polarization vector normal to the grain boundary is equal for grain A and grain B, as shown in (b). (c) shows discontinuity of polarization where the component of the polarization vector along the grain boundary normal is not equal on either side of the boundary leading to uncompensated charge as shown in (d). Image reprinted from Acta Materialia, 128, Mantri et. al., Ferroelectric Domain Continuity over grain boundaries, 400-405, 2017, with permission from Elsevier [26].

Construction of Modelled Microstructure

To study domain percolation in a polycrystal, all five dimensions for each grain boundary are required, i.e., the misorientation between the neighboring grains as well as the grain boundary plane normal.

For a polycrystal with "n" grains, n random points are selected in a cube to represent the grain body centers. To generate the microstructure, the Voronoi tessellation approach is taken. Points that are equidistant to neighboring grain centers are assigned to the grain boundary. Grain boundary plane normals are calculated through least squares fitting of the grain boundary points that belong to a particular grain-grain boundary. Depending on the model type, the unit cell orientation of each grain is either randomly assigned, aligned with a probability to an external axis (textured), or given specific orientation relationships with neighboring grains (weighted grain boundary populations). A sample polycrystal of 1000 grains is shown in Figure 3(a). To model fiber texture in our polycrystals, the March-Dollase distribution [33] is used to create a preferred crystallographic direction in the polycrystal. To increase the population of $\sum 3$ grain boundaries in the model microstructure, a fraction of the grains are given $\sum 3$ misorientation (60° rotation about$< 111 >$) with respect to a neighboring grain, prior to random assignment of remaining orientations.

The ferroelectric symmetry studied in this paper is tetragonal. Tetragonal ferroelectrics can have 6 possible polarization directions along any of the <100> axes and 3 possible spontaneous strain states, as opposing polarization directions have an identical strain tensor. The domain walls for 90° domains in tetragonal ferroelectrics are on the {110} crystallographic planes [4]. Complicated domain structures like herringbone, watermark and square-net can form in ferroelectric materials. Here, an alternating stripe domain structure with 90° domain walls is used, as this is most commonly observed [34,35]. Hence, the continuity of two alternating domains (i.e., the repeating unit of the alternating stripe domain structure) over the

grain boundary is studied. These results can be extended to any number of multiples of the repeating unit and hence, are applicable for any domain density of the striped domain structure.

While applying the domain continuity conditions, first the domain walls are matched within a chosen angular tolerance. If successful matching occurs, then the residual polarization charge on the grain boundary is calculated. As the continuity of a striped-domain structure is being considered, residual charge is calculated as the sum of the modulus of the residual charge created at the grain boundary for each domain. If this charge falls below a chosen tolerance, domain continuity through the grain boundary is considered successful. These tolerance values effectively allow for true grain boundary variations such as space charge and dislocation densities to be accommodated. Geometric mismatch angular tolerance is studied in the range of 5 - 15°. The figure of 15° comes from twist deviation angles observed by Tsurekawa et. al. for grain boundaries permitting continuity [18]. In addition to this, 15° is considered an acceptable higher tolerance in texts [36,37] related to slip plane continuity for transgranular plastic deformation, a geometrically analogous process. Residual grain boundary polarization charge tolerance is studied in the range of 0.1Ps to 1.5Ps. This implies a maximum charge tolerance of 0.75Ps per domain. A head-to-head polarization creates a residual charge of $2P_S$. Spontaneous polarization of barium titanate in its room temperature phase [38–40] is around $26\ \mu C/cm^2$, which equates to an equivalent screening charge created by an oxygen vacancy concentration of $16 \times 10^{13}\ vacancies/cm^2$ at the grain boundary.

Results

Figure 3(a) shows a modelled random polycrystal of 1000 grains (see Methods for more information). To begin the percolation process, a grain is chosen at random and is assigned a random tetragonal stripe domain configuration. All the neighboring grains to this grain are checked for domain continuity using the geometrical plane matching and polarization charge continuity at the grain boundary plane. The domain transmits through all of its grain boundaries that satisfy the condition under the charge and angular tolerance set. The same process is then repeated for each of the neighboring grains to which the domain structure has transmitted by checking for domain continuity with their respective neighbors. Using this method, domain walls can be seen to percolate through the polycrystal with a web like structure starting from the grain where domain nucleation occurred. An example is shown in Figure 3(b). The grain center marked with the bigger black sphere is the initiation grain. This grain had 12 neighbors. Only one neighbor, however, allowed domain percolation within acceptable angular and charge tolerance and is shown by the single connecting thread. In some cases, domain walls from a single grain can pass into more than one neighboring grain, thus the connecting threads tend to branch. The number of grain boundaries that a thread crosses has been called here as the domain percolation length for that thread. The total percolation i.e., the spread of the domain percolation web is the total number of grains that domains percolate through for a given nucleation point. In Figure 3(b), the total percolation or the spread of the percolation web is 16 grain boundaries. The percolation length is defined here as the largest number of grain boundaries traversed from one point on the web to another. In this case thread 4 and thread 6 in total form the longest thread with a percolation length of 9 grain boundaries.

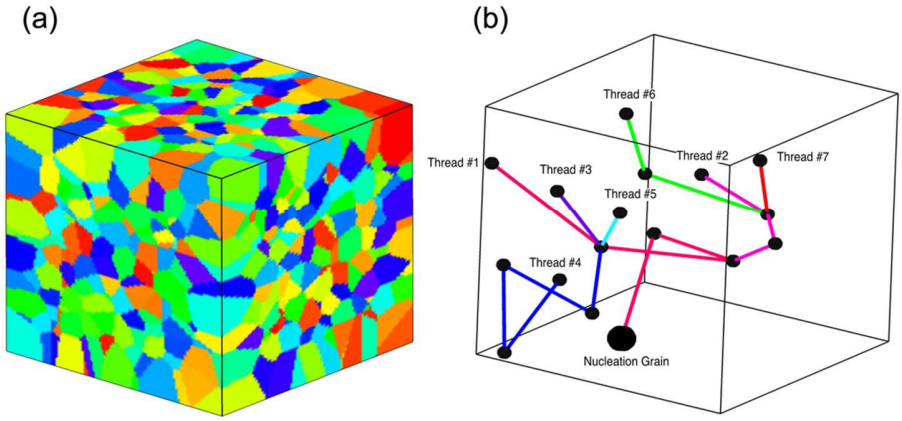

Figure 4. (a) a 1000-grain microstructure generated using the Voronoi tessellation method. (b) a subsection of a microstructure showing the domain percolation starting from the grain marked by the bigger black sphere and spreading through the microstructure via threads. Each dot represents the centroid of a grain through which the domain structure has percolated.

Variation with seed grain

The domain percolation web as well as it's attributes, the domain percolation length and the domain percolation spread, will change as a function of the nucleating grain due to statistical chance of assigning orientations to grains. Figure 4 shows the domain percolation spread as a function of nucleating grain for a polycrystal of 50 randomly oriented grains for the case of 10° angular tolerance and $1P_S$ charge tolerance. The histogram for the frequency of observing a particular domain percolation length for this example is shown in the inset in Figure 4. Figure 4 shows that occasionally there can be a grain which is not fit to propagate the domains (hence very low domain percolation). As any grain can be the nucleating grain, the average domain percolation length has been used as representative of the domain percolation for a particular polycrystal. To further improve the statistical significance, 100 unique microstructures are generated for each condition investigated, with the final reported values being the average of those found across the 100 microstructures.

Percolation for varying angular and charge tolerances

Figure 5 shows the domain percolation spread for different angular tolerances and charge tolerances. In general (see case 5° angular tolerance), as the charge tolerance increases the domain percolation increases with practically no percolation observed for $0.1P_s$ charge tolerance. For the case of 5° angular tolerance, increasing the charge tolerance from $0.5P_S$ to $1P_S$ increases the domain percolation by 423%. The case of $0.5P_s$ charge tolerance is a good example showing the effect of angular tolerance with a 376% increase in percolation on changing the angular tolerance from 5° to 10°. However, for higher angular and charge tolerances, no change in domain percolation is visible. For example, when the tolerances increase to 10 ° and 1 P_s, domain percolation saturates. To check if the percolation saturation was due to increases in domain percolation under high tolerances or due to percolating domain walls hitting the microstructure model boundaries as a dead end, larger microstructures were studied. Domain percolations was studied in 50 grains, 100 grains, 200 grains, and 300 random microstructures under the angular tolerance of 10° and charge tolerance of 1 P_s. The inset in Figure 5 shows the total domain percolation spread comparison. For higher tolerances, the domain percolation web spreads across the entire microstructure. The percentage of grains with percolated domains is greater than 97%, and therefore higher tolerance values do not affect the percolation length anymore.

Percolation length for microstructures with crystallographic texture and preferred grain boundary populations

In addition to being affected by the angular and charge tolerances, domain percolation has been shown to be affected by the grain boundary character i.e., the grain – grain orientation distribution and the grain boundary plane normal distribution [26,27]. In this study, control over grain boundary plane normals cannot be exercised as they are generated geometrically via the microstructure generation process. Control over the remaining three dimensions of grain boundaries is studied by

two methods: 1) creating a preferred ∑3 grain boundary population, and 2) by introducing crystallographic texture. These two methods are different in the sense that in the case of ∑3 preferred grain boundary population, a percentage of neighbors are chosen and the orientation (of the two grains forming the neighboring group) relative to each other is changed to ∑3. This does not introduce crystallographic texture to the material as the set of neighboring groups are still randomly oriented with respect to any external axis. However, in case of texturing, a percentage of grains (not necessarily neighbors) are chosen and their orientation is changed such that the microstructure is crystallo-graphically textured along a particular global axis, in this case either the [100] or the [111] axis of those grains is preferentially aligned to the vertical direction of the microstructure model.

Figure 6 shows the effect of varying percentages of ∑3 grain boundary population on the domain percolation. Two angular and two charge tolerances were studied for polycrystals with 1% and 13% ∑3 favored grain boundary populations. For a numerical perspective, a 50-grain microstructure would have around 250 grain boundaries i.e., grain -grain combinations, out of which 1% would mean ~2or 3 neighboring grain combinations being ∑3 and 13% would mean 35-40 neighboring grain combinations to be ∑3 misoriented with respect to each other. For smaller tolerances (5° and $0.5P_S$), the percentage of ∑3 grain boundaries influenced the domain percolation length, increasing by 71% on changing the ∑3 grain boundary population from 1% to 13%. As tolerances are increased, the effect of changing ∑3 grain boundary population decreases. For larger tolerances (angle>10° and/or charge>1 P_s), there is no visible effect of changing the grain boundary population. This again, however, is related to the fact that at larger tolerances, the full microstructure is percolated, saturating the achievable percolation length. Note that larger ∑3 grain boundary population was not possible while maintaining the non-∑3 population percentage.

Figure 7 shows the effect of crystallographic texturing on domain percolation. Fiber texture is introduced into the model polycrystal by weighting grain orientations using the March Dollase (MD) [33] which has been demonstrated to accurately describe texture in ferroelectric materials fabricated using template methods [41]. Textures along the [100] axis and [111] axis were studied. All grains were textured. The MD 'r' parameter[33] specifies the degree of texture. It varies between [0,1] with smaller values representing a stronger texture and 1 representing a random polycrystal. Here, two values of 'r' was studied. Two angular tolerances and two charge tolerances were studied. For the case of r=0.5, not much difference in the domain percolation between the two axes is observed. However, when we reduced the r to 0.1 (highly textured), domain percolation increased by 220% for the tolerance of 5°, $0.5P_S$ for the [100] textured microstructure (shown in the inset of Figure 7). Not such a large difference (~1% increase) was observed for the [111] textured microstructure. This can be expected as the tetragonal symmetry of the ferroelectric is being studied, with polarization direction along <100> that is perpendicular to the {110} domain walls. Similar to the previous case of preferred ∑3 grain boundary population, for lower tolerances, increasing the degree of texture (decreasing the r), increases the domain percolation length. The effect of 'r', however, becomes negligible at higher tolerance values as the model is completely percolated.

Finally, a comparison of domain percolation in random polycrystals, preferred ∑3 grain boundary population, and textured polycrystals is shown in Figure 8. This figure highlights the impact of these microstructural changes at low angular and charge tolerance levels. When the grain boundary tolerance level for charge and angular mismatch is low (5°, $0.5P_S$), the microstructural changes of increasing the percentage of ∑3 grain boundaries and texturing can increase the domain percolation length significantly. However, in microstructures that can accommodate larger angular and charge tolerances, the domain percolation length changes are not very high as the microstructure would be close to fully percolated without changes in the grain boundary population or texturing. It should be pointed out that the effect of texturing along [100] is larger than increasing the preferred ∑3 grain boundary population.

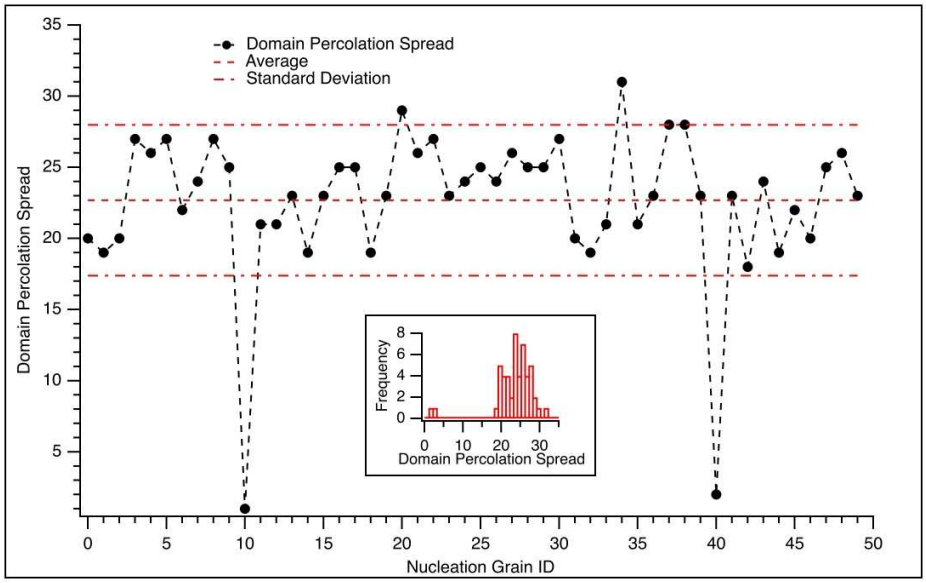

Figure 5: This figure shows the variation in domain percolation as a function of different nucleation points in the same polycrystal of 50 grains. The x axis is the nucleating grain ID and the y axis is the corresponding domain percolation. Inset: frequency histogram for the number of grains that lead to the same domain percolation. The tolerances for this case are 10° and 1Ps.

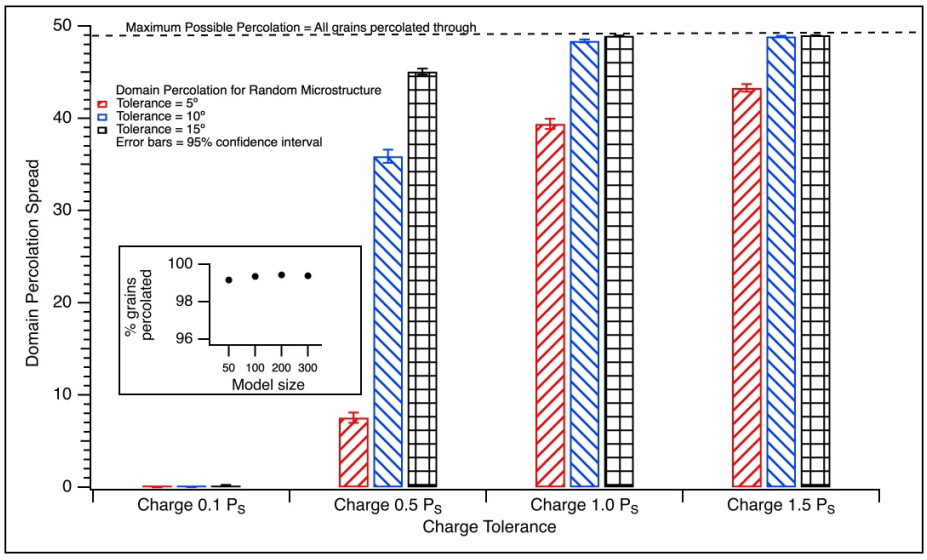

Figure 6: Frequency histograms of domain percolation for 100 different-50 grain random polycrystals as a function of varying geometric mismatch angle and residual grain boundary charge tolerances. Inset: A comparison of domain percolation spread (y-axis is the percentage of grains through with domains percolate) for modelled polycrystals with 50, 100, 200, and 300 grains for the angular tolerance of 10° and charge tolerance of 1 P_s. For tolerance as high as 10° and 1 P_s, domain percolation covers the entire microstructure. Therefore, changes in domain percolation at these tolerances are unlikely.

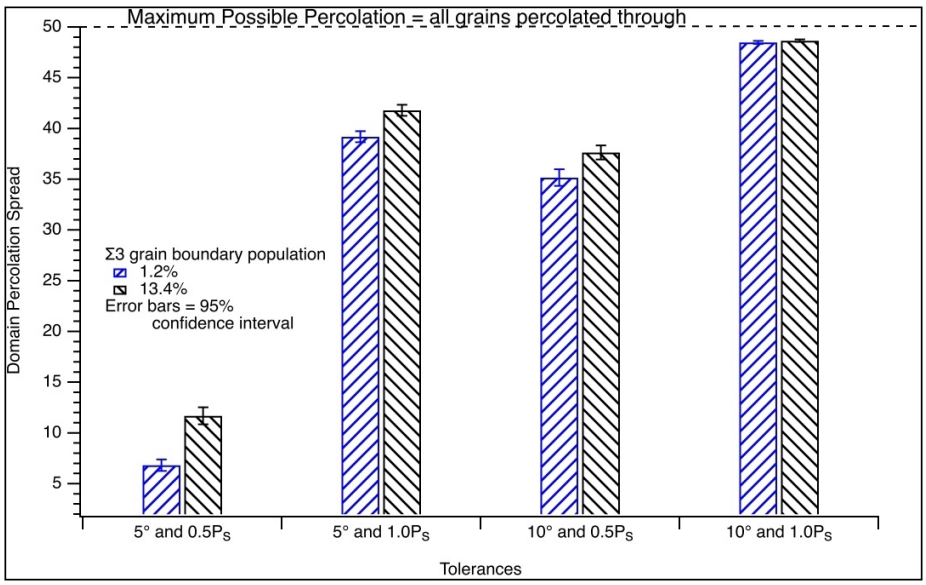

Figure 7: The effect of preferred ∑3 grain boundary character percentage (~1% and ~13%) on domain percolation studied for different charge and angular tolerances.

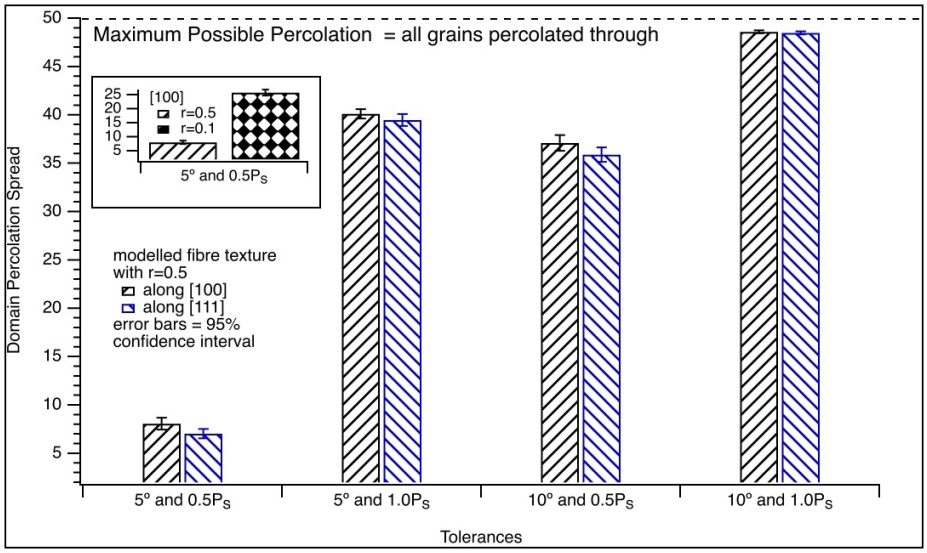

Figure 8: The effect of fibre texture modelled using the March Dollase function [33] *studied for varying charge and angular tolerances. Texture along [100] and [111] axes was studied. Inset: Two values of MD 'r' parameter studied show a 220% jump in domain percolation for the 5 °and 0.5P_S case.*

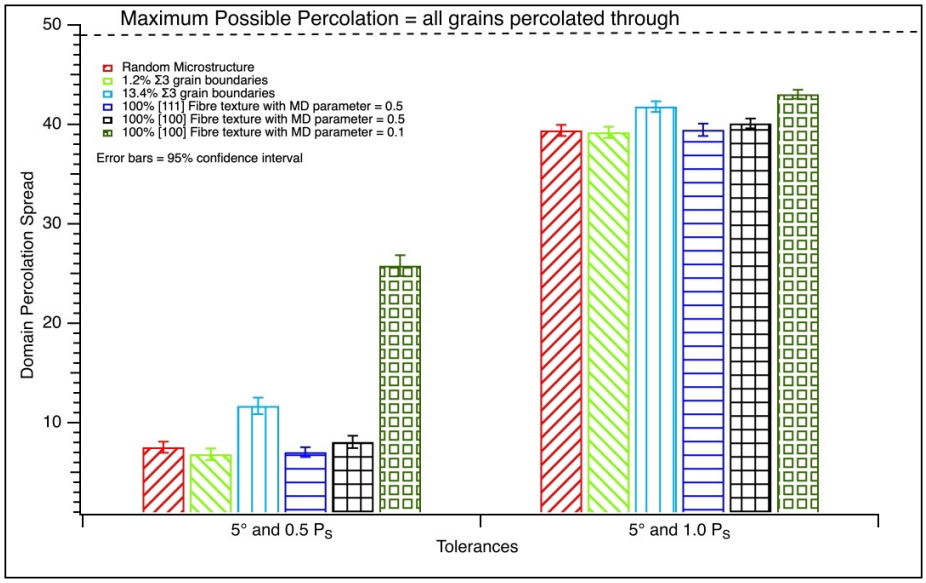

Figure 9: A comparison of domain percolation in the case of random microstructure, ~1% ∑3 grain boundary character, ~13 % ∑3 grain boundary character, [111] fibre texture with r=0.5, [100] fibre texture with r=0.5, and [100] fibre texture with r=0.1 for the case of 5°, 0.5 P_s and 5°, 1P_s tolerance respectively.

Discussion

The results presented above provide valuable insight to the long-observed phenomena of domain walls traversing grain boundaries in polycrystalline ferroelectric materials. It has been demonstrated that even in polycrystalline systems with randomly orientated grains and random grain boundary populations, as well as tight tolerances on the domain wall plane matching angle and uncompensated polarization charge (5° and 0.5 P_S), percolation of domain walls through multiple grain boundaries is expected. The percolation lengths are drastically increased even with modest relaxing of the tolerance values. At an angular tolerance of 15° and/or a charge compensation of 1.0 P_S, domain walls are expected to percolate the entire polycrystal.

Given prior experimental observations of domain wall continuity through grain boundaries are limited to 2D surface interrogation methods, it is likely that domain percolation is commonplace in most polycrystalline ferroelectrics. Increasing percolation lengths in randomly oriented microstructures will depend on the ability of the grain boundary to compensate the residual polarization charge and strain mismatch. In addition to grain boundary space charge developed during sintering, mobility of dopants and defects from the bulk to the grain boundary during domain formation will also impact the tolerances thereby affecting domain percolation lengths. The residual grain boundary charge continuity equation would change if there were some charges already present to compensate for the residual charge created by domain continuity. This charge can be the grain boundary space charge already created by accumulation of charged defects at the grain boundary at the sintering temperature when the microstructure is forming [42]. This charge could also come from the mobility of charged dopants/defects at the Curie temperature in the ferroelectric when the domains are forming. Thus, ferroelectrics with higher Curie point and higher dopant/defect mobility would potentially provide better conditions for domain percolation. Therefore, it can be said that $BiFeO_3$ [43] (T_C ~ 830°C) would be more likely than $BaTiO_3$[2] (T_C ~ 120°C) to form longer length-scale domain percolation networks. Another interesting point to note is that keeping the grain boundary normal and the angular mismatch between the perpendicular component of the polarization of neighboring grains same, the residual charge created at the grain boundary changes as a function of spontaneous polarization i.e., for the same angular incompatibility, ferroelectric domain percolation would be less likely for $PbTiO_3$ [44] (P_S = 85 $\mu C/cm^2$) than $BaTiO_3$ (P_S =

26 $\mu C/cm^2$). In other words, higher charge compensation would be required in systems with high spontaneous polarization if domain percolation were to take place.

Beyond pure compositional control, it has been shown that manipulating the microstructure of the material by either; 1) increasing the grain boundary population with more $\sum 3$ type boundaries, or 2) inducing crystallographic texture, further increases the probability and length-scale of domain percolation. Crystallographic texturing is commonly applied to these materials through templated grain growth strategies, and thus can be induced relatively easily. It should be acknowledged, however, that any type of heterogeneous templating will add complexity to the domain structures within the grains. Weighting of grain boundary populations, while likely occurring due to non-equal grain boundary energies during sintering, is more difficult to control. In common perovskites like $SrTiO_3$, $BaTiO_3$, $PbZr_xTi_{1-x}O_3$, $\sum 3$ type boundaries have been shown to be more common [31,32], however methods to control these weightings are not described in the literature. The pathway to this will lie in sintering methods for ceramics. Spark plasma [45], two step [46], conventional and microwave sintering [47] together with compositional control may allow weighted grain boundary populations to be varied. However, one of the biggest restrictions to weighted grain boundary control is the lack of experimental methods to measure large-scale microstructures. Atom probe tomography (APT) [48] and focused ion beam sectioning with electron back scattered diffraction (EBSD, FIB-SEM) [49–52] provide high resolution orientational information for grain boundaries but are limited by the sample size and acquisition times. Developments in three-dimensional x-ray diffraction (3D-XRD) [53] using modern synchrotron sources and high-speed detectors offers the most promise for achieving this, with surveys of many 10,000's of grain boundaries possible.

Our results represent those from an ideal case. In real materials there are many additional variables that may influence the magnitude of the domain percolation. Firstly, a single grain boundary may not be flat, it would need to be modelled as many smaller planes with different normals. This would imply that a single grain boundary could vary from allowing perfect plane matching and polarization continuity, to becoming a dielectric dead layer with a high depolarizing field. Such energetically unfavorable structures have been observed to create a polar vortex structure within the grain[54,55]. Thus, grain boundary thickness, dielectric characteristics and polarization orientations can affect the domain structure within the grain, potentially effecting ongoing percolation. It should also be acknowledged that we have not incorporated any effect of the grain size. In fact, the interplay between grain size and grain boundary thickness is also known to change the domain structure as well as change the effect of external stimuli on the system [56]. The true impact of these more complex characteristics of the microstructure will only be able to be investigated with high-resolution experimental maps of the microstructures. The current results are also restricted to tetragonal symmetry. We can expect the domain percolation lengths to further increase in rhombohedral and orthorhombic on account of the increased number of domain types as was shown for bi-crystals of these symmetries [27]. It would be interesting to predict domain percolation in systems with co-existence of multiple phases, for example, $PbZr_xTi_{1-x}O_3$ at the morphotropic phase boundary[57] with the coexistence of tetragonal, rhombohedral, and monoclinic phases.

By controlling the length-scales of percolation, many phenomena that may be influenced by it can be investigated. In the case of polycrystalline ferroelectrics that are used as piezoelectrics, domain wall motion is strongly related to the maximum achievable electric-field-induced strains. Previous work has suggested that domain walls traversing grain boundaries may inhibit motion due to pinning, but others have suggested that the percolation of domain walls will encourage correlated response, potentially improving properties [10,19,24,25]. Other properties are also intimately linked to the length scales of domain percolation. Many ferroelectric systems such as $BiFeO_3$ [58,59], $BaTiO_3$ [60] , $ErMnO_3$ [61] have been shown to have conducting domain walls in an otherwise insulating matrix. Ionic/electronic charge could potentially move on length-scales spanning many grains when the conducting domain walls are continuous over grain boundaries. The potential to manipulate this length-scale may offer methods for tuning unique electrical and electro-mechanical properties of these materials [62]. Beyond ferroelectrics, ferroelastic materials such as shape memory alloys may also find their properties dependent on the magnitude of domain wall percolation lengths, while the methods developed here are also transferrable to other planar continuity phenomena such as slip transfer in ductile metals [37].

Conclusions

In this work, we have studied domain percolation in a modelled polycrystal ferroelectric of tetragonal symmetry. The domain structure studied is alternating stripe domains of the 90° type. Domain percolation is quantified by the number of grain boundaries that domain walls can traverse through in a given microstructure. Different grain boundary angular mismatch tolerances and residual grain boundary polarization charge tolerances were studied. The effect of a preferred grain boundary population of ∑3 grain boundaries and fiber texture on domain percolation was also studied. It was found that increasing the tolerances, preferred ∑3 grain boundary as well as fiber texturing, all have the same qualitative effect of increasing the domain percolation lengths in a microstructure. The effect of grain boundary tolerances is very high with the domain percolation increasing by 376% on increasing the angular tolerance from 5° to 10° at a charge tolerance of $0.5P_S$ with greater then 90% domain percolation in the modelled microstructure when tolerances higher than 10° and $1P_S$ are possible. However, at lower grain boundary tolerances, the ∑3 preferred grain boundary population and [100] texturing can increase the domain percolation by as much as 55% and 243% respectively. Using the results of this paper as guidance, the control of length-scales of continuously percolating domain structures across a polycrystalline microstructure is possible using processing parameters that impact the preferred grain boundary types and texture of the material. These continuous domains can potentially change the piezoelectric properties by modifying the impact of grain boundary pinning on domain wall motion, or the magnitude of correlated domain wall motion between neighboring grains. In addition to ferroelectric materials and their elastic counterparts – ferroelastic materials, this study can also be applied to other material phenomena wherein planar interactions with grain boundaries are significant.

Acknowledgements

This project was in part supported by the Australian Federal Government through the Next Generation Technologies Fund, the DST Strategic Research Initiative in Advanced Materials and Sensors, the US Office of Naval Research (award number N62909-19-1-2090) and by the Australian Research Council Centre of Excellence in Future Low-Energy Electronics Technologies (project number CE170100039) funded by the Australian Government.

References

[1] T. Mitsui, I. Tatsuzaki, E. Nakamura, An Introduction to the Physics of Ferroelectrics, Gordon and Breach Science Publishers, 1976.

[2] M. E. Lines, A. M. Glass, Principles and Applications of Ferroelectrics and Related Materials, Oxford University Press, 2001.

[3] J. Fousek, V. Janovec, The Orientation of Domain Walls in Twinned Ferroelectric Crystals, J Appl Phys. 40 (1969) 135–142. https://doi.org/10.1063/1.1657018.

[4] S. Mantri, J. Daniels, Domain walls in ferroelectrics, Journal of the American Ceramic Society. 104 (2021) 1619–1632. https://doi.org/https://doi.org/10.1111/jace.17555.

[5] H. Simons, A.B. Haugen, A.C. Jakobsen, S. Schmidt, F. Stöhr, M. Majkut, C. Detlefs, J.E. Daniels, D. Damjanovic, H.F. Poulsen, Long-range symmetry breaking in embedded ferroelectrics, Nat Mater. 17 (2018) 814–819. https://doi.org/10.1038/s41563-018-0116-3.

[6] P.S. Bednyakov, B.I. Sturman, T. Sluka, A.K. Tagantsev, P. v Yudin, Physics and applications of charged domain walls, NPJ Comput Mater. 4 (2018). https://doi.org/10.1038/s41524-018-0121-8.

[7] W.R. Cook, Domain Twinning in Barium Titanate Ceramics, Journal of the American Ceramic Society. 39 (1956) 17–19. https://doi.org/10.1111/j.1151-2916.1956.tb15592.x.

[8] P.W. Forsbergh, Domain Structures and Phase Transitions in Barium Titanate, Physical Review. 76 (1949) 1187–1201. https://doi.org/10.1103/PhysRev.76.1187.

[9] R. C. DeVries, J. E. Burke, Microstructure of Barium Titanate Ceramics, Journal of the American Ceramic Society. (1957) 200–206.

[10] G. Arlt, P. Sasko, Domain configuration and equilibrium size of domains in BaTiO3 ceramics, J Appl Phys. 51 (1980) 4956–4960. https://doi.org/10.1063/1.328372.

[11] D. Damjanovic, M. Demartin, The Rayleigh law in piezoelectric ceramics, J Phys D Appl Phys. 29 (1996) 2057–2060. https://doi.org/10.1088/0022-3727/29/7/046.

[12] A. Pramanick, D. Damjanovic, J.E. Daniels, J.C. Nino, J.L. Jones, Origins of Electro-Mechanical Coupling in Polycrystalline Ferroelectrics During Subcoercive Electrical Loading, Journal of the American Ceramic Society. 94 (2011) 293–309. https://doi.org/10.1111/j.1551-2916.2010.04240.x.

[13] J.L. Jones, M. Hoffman, J.E. Daniels, A.J. Studer, Direct measurement of the domain switching contribution to the dynamic piezoelectric response in ferroelectric ceramics, Appl Phys Lett. 89 (2006) 092901. https://doi.org/10.1063/1.2338756.

[14] D. Damjanovic, Logarithmic frequency dependence of the piezoelectric effect due to pinning of ferroelectric-ferroelastic domain walls, Phys Rev B. 55 (1997) R649–R652. https://doi.org/10.1103/PhysRevB.55.R649.

[15] J.F. Scott, M. Dawber, Oxygen-vacancy ordering as a fatigue mechanism in perovskite ferroelectrics, Appl Phys Lett. 76 (2000) 3801–3803. https://doi.org/10.1063/1.126786.

[16] A. Kontsos, C.M. Landis, Computational modeling of domain wall interactions with dislocations in ferroelectric crystals, Int J Solids Struct. 46 (2009) 1491–1498. https://doi.org/10.1016/j.ijsolstr.2008.11.021.

[17] Y.-M. Chiang, T. Takagi, Grain-Boundary Chemistry of Barium Titanate and Strontium Titanate: I, High-Temperature Equilibrium Space Charge, Journal of the American Ceramic Society. 73 (1990) 3278–3285. https://doi.org/10.1111/j.1151-2916.1990.tb06450.x.

[18] S. Tsurekawa, K. Ibaraki, K. Kawahara, T. Watanabe, The continuity of ferroelectric domains at grain boundaries in lead zirconate titanate, Scr Mater. 56 (2007) 577–580. https://doi.org/https://doi.org/10.1016/j.scriptamat.2006.12.029.

[19] H. Takahashi, Y. Numamoto, J. Tani, S. Tsurekawa, Domain Properties of High-Performance Barium Titanate Ceramics, Jpn J Appl Phys. 46 (2007) 7044–7047. https://doi.org/10.1143/jjap.46.7044.

[20] G. Arlt, Twinning in ferroelectric and ferroelastic ceramics: stress relief, J Mater Sci. 25 (1990) 2655–2666. https://doi.org/10.1007/BF00584864.

[21] T. O'Reilly, K. Holsgrove, A. Gholinia, D. Woodruff, A. Bell, J. Huber, M. Arredondo, Exploring domain continuity across BaTiO3 grain boundaries: theory meets experiment, Acta Mater. (2022) 118096. https://doi.org/10.1016/j.actamat.2022.118096.

[22] H. Takahashi, Y. Numamoto, J. Tani, S. Tsurekawa, Considerations for BaTiO3 Ceramics with High Piezoelectric Properties Fabricated by Microwave Sintering Method, Jpn J Appl Phys. 47 (2008) 8468–8471. https://doi.org/10.1143/jjap.47.8468.

[23] S. Wicks, K. Seal, S. Jesse, V. Anbusathaiah, S. Leach, R. Edwin Garcia, S. v Kalinin, V. Nagarajan, Collective dynamics in nanostructured polycrystalline ferroelectric thin films using local time-resolved measurements and switching spectroscopy, Acta Mater. 58 (2010) 67–75. https://doi.org/https://doi.org/10.1016/j.actamat.2009.08.057.

[24] D.M. Marincel, H. Zhang, A. Kumar, S. Jesse, S. v. Kalinin, W.M. Rainforth, I.M. Reaney, C.A. Randall, S. Trolier-McKinstry, Influence of a Single Grain Boundary on Domain Wall Motion in Ferroelectrics, Adv Funct Mater. 24 (2014) 1409–1417. https://doi.org/10.1002/adfm.201302457.

[25] D.M. Marincel, H.R. Zhang, J. Britson, A. Belianinov, S. Jesse, S. v. Kalinin, L.Q. Chen, W.M. Rainforth, I.M. Reaney, C.A. Randall, S. Trolier-Mckinstry, Domain pinning near a single-grain boundary in tetragonal and rhombohedral lead zirconate titanate films, Phys Rev B Condens Matter Mater Phys. 91 (2015). https://doi.org/10.1103/PhysRevB.91.134113.

[26] S. Mantri, J. Oddershede, D. Damjanovic, J.E. Daniels, Ferroelectric domain continuity over grain boundaries, Acta Mater. 128 (2017). https://doi.org/10.1016/j.actamat.2017.01.065.

[27] S. Mantri, J.E. Daniels, Ferroelectric domain continuity over grain boundaries for tetragonal, orthorhombic and rhombohedral crystal symmetries, IEEE Trans Ultrason Ferroelectr Freq Control. (2018). https://doi.org/10.1109/TUFFC.2018.2827406.

[28] Y. Chang, J. Wu, Z. Liu, E. Sun, L. Liu, Q. Kou, F. Li, B. Yang, W. Cao, Grain-Oriented Ferroelectric Ceramics with Single-Crystal-like Piezoelectric Properties and Low Texture Temperature, ACS Appl Mater Interfaces. 12 (2020) 38415–38424. https://doi.org/10.1021/acsami.0c11680.

[29] M.J. Hoffmann, H. Kungl, High strain lead-based perovskite ferroelectrics, Curr Opin Solid State Mater Sci. 8 (2004) 51–57. https://doi.org/https://doi.org/10.1016/j.cossms.2003.12.003.

[30] A.B. Haugen, M.I. Morozov, J.L. Jones, M.-A. Einarsrud, Rayleigh analysis of dielectric properties in textured K0.5Na0.5NbO3 ceramics, J Appl Phys. 116 (2014) 214101. https://doi.org/10.1063/1.4902858.

[31] F. Ernst, M.L. Mulvihill, O. Kienzle, M. Rühle, Preferred Grain Orientation Relationships in Sintered Perovskite Ceramics, Journal of the American Ceramic Society. 84 (2004) 1885–1890. https://doi.org/10.1111/j.1151-2916.2001.tb00931.x.

[32] D.M. Saylor, B. Dasher, T. Sano, G.S. Rohrer, Distribution of Grain Boundaries in SrTiO3 as a Function of Five Macroscopic Parameters, Journal of the American Ceramic Society. 87 (2004) 670–676. https://doi.org/10.1111/j.1551-2916.2004.00670.x.

[33] W.A. Dollase, Correction of intensities for preferred orientation in powder diffractometry: application of the March model, J Appl Crystallogr. 19 (1986) 267–272. https://doi.org/10.1107/S0021889886089458.

[34] J.A. Hooton, W.J. Merz, Etch Patterns and Ferroelectric Domains in BaTiO3 Single Crystals, Physical Review. 98 (1955) 409–413. https://doi.org/10.1103/PhysRev.98.409.

[35] A. Renuka Balakrishna, J.E. Huber, I. Münch, Nanoscale periodic domain patterns in tetragonal ferroelectrics: A phase-field study, Phys Rev B. 93 (2016) 174120. https://doi.org/10.1103/PhysRevB.93.174120.

[36] K.G. Davis, E. Teghtsoonian, A. Lu, Slip band continuity across grain boundaries in aluminum, Acta Metallurgica. 14 (1966) 1677–1684. https://doi.org/https://doi.org/10.1016/0001-6160(66)90020-4.

[37] E. Bayerschen, A.T. McBride, B.D. Reddy, T. Böhlke, Review on slip transmission criteria in experiments and crystal plasticity models, J Mater Sci. 51 (2016) 2243–2258. https://doi.org/10.1007/s10853-015-9553-4.

[38] Y.L. Li, L.E. Cross, L.Q. Chen, A phenomenological thermodynamic potential for BaTiO3 single crystals, J Appl Phys. 98 (2005) 064101. https://doi.org/10.1063/1.2042528.

[39] H.H. Wieder, Electrical Behavior of Barium Titanate Single Crystals at Low Temperatures, Physical Review. 99 (1955) 1161–1165. https://doi.org/10.1103/PhysRev.99.1161.

[40] M.E. Drougard, R. Landauer, D.R. Young, Dielectric Behavior of Barium Titanate in the Paraelectric State, Physical Review. 98 (1955) 1010–1014. https://doi.org/10.1103/PhysRev.98.1010.

[41] S.-B. Lee, T.S. Key, Z. Liang, R.E. García, S. Wang, X. Tricoche, G.S. Rohrer, Y. Saito, C. Ito, T. Tani, Microstructure design of lead-free piezoelectric ceramics, J Eur Ceram Soc. 33 (2013) 313–326. https://doi.org/https://doi.org/10.1016/j.jeurceramsoc.2012.08.015.

[42] Y.-M. Chiang, T. Takagi, Grain-Boundary Chemistry of Barium Titanate and Strontium Titanate: II, Origin of Electrical Barriers in Positive-Temperature-Coefficient Thermistors, Journal of the American Ceramic Society. 73 (1990) 3286–3291. https://doi.org/10.1111/j.1151-2916.1990.tb06451.x.

[43] R. Palai, R.S. Katiyar, H. Schmid, P. Tissot, S.J. Clark, J. Robertson, S.A.T. Redfern, G. Catalan, J.F. Scott, β phase and γ–β metal-insulator transition in multiferroic BiFeO3, Phys Rev B. 77 (2008) 014110. https://doi.org/10.1103/PhysRevB.77.014110.

[44] R.J. Nelmes, W.F. Kuhs, The crystal structure of tetragonal PbTiO3 at room temperature and at 700 K, Solid State Commun. 54 (1985) 721–723. https://doi.org/10.1016/0038-1098(85)90595-2.

[45] Z.A. Munir, U. Anselmi-Tamburini, M. Ohyanagi, The effect of electric field and pressure on the synthesis and consolidation of materials: A review of the spark plasma sintering method, J Mater Sci. 41 (2006) 763–777. https://doi.org/10.1007/s10853-006-6555-2.

[46] N.J. Lóh, L. Simão, C.A. Faller, A. de Noni, O.R.K. Montedo, A review of two-step sintering for ceramics, Ceram Int. 42 (2016) 12556–12572. https://doi.org/https://doi.org/10.1016/j.ceramint.2016.05.065.

[47] M. Oghbaei, O. Mirzaee, Microwave versus conventional sintering: A review of fundamentals, advantages and applications, J Alloys Compd. 494 (2010) 175–189. https://doi.org/https://doi.org/10.1016/j.jallcom.2010.01.068.

[48] B. Gault, A. Chiaramonti, O. Cojocaru-Mirédin, P. Stender, R. Dubosq, C. Freysoldt, S.K. Makineni, T. Li, M. Moody, J.M. Cairney, Atom probe tomography, Nature Reviews Methods Primers. 1 (2021) 51. https://doi.org/10.1038/s43586-021-00047-w.

[49] A.D. Rollett, S.-B. Lee, R. Campman, G.S. Rohrer, Three-Dimensional Characterization of Microstructure by Electron Back-Scatter Diffraction, Annu Rev Mater Res. 37 (2007) 627–658. https://doi.org/10.1146/annurev.matsci.37.052506.084401.

[50] D.J. Rowenhorst, A. Gupta, C.R. Feng, G. Spanos, 3D Crystallographic and morphological analysis of coarse martensite: Combining EBSD and serial sectioning, Scr Mater. 55 (2006) 11–16. https://doi.org/https://doi.org/10.1016/j.scriptamat.2005.12.061.

[51] M.D. Uchic, L. Holzer, B.J. Inkson, E.L. Principe, P. Munroe, Three-Dimensional Microstructural Characterization Using Focused Ion Beam Tomography, MRS Bull. 32 (2007) 408–416. https://doi.org/10.1557/mrs2007.64.

[52] S. Zaefferer, S.I. Wright, D. Raabe, Three-Dimensional Orientation Microscopy in a Focused Ion Beam–Scanning Electron Microscope: A New Dimension of Microstructure Characterization, Metallurgical and Materials Transactions A. 39 (2008) 374–389. https://doi.org/10.1007/s11661-007-9418-9.

[53] H.F. Poulsen, X. Fu, E. Knudsen, E.M. Lauridsen, L. Margulies, S. Schmidt, 3DXRD – Mapping Grains and Their Dynamics in 3 Dimensions, Materials Science Forum. 467–470 (2004) 1363–1372. https://doi.org/10.4028/www.scientific.net/MSF.467-470.1363.

[54] Y. Su, N. Liu, G.J. Weng, A phase field study of frequency dependence and grain-size effects in nanocrystalline ferroelectric polycrystals, Acta Mater. 87 (2015) 293–308. https://doi.org/10.1016/j.actamat.2015.01.015.

[55] Y. Su, H. Kang, Y. Wang, J. Li, G.J. Weng, Intrinsic versus extrinsic effects of the grain boundary on the properties of ferroelectric nanoceramics, Phys Rev B. 95 (2017) 054121. https://doi.org/10.1103/PhysRevB.95.054121.

[56] M.T. Buscaglia, M. Viviani, V. Buscaglia, L. Mitoseriu, A. Testino, P. Nanni, Z. Zhao, M. Nygren, C. Harnagea, D. Piazza, C. Galassi, High dielectric constant and frozen macroscopic polarization in dense nanocrystalline BaTiO3 ceramics, Phys Rev B. 73 (2006) 064114. https://doi.org/10.1103/PhysRevB.73.064114.

[57] B. Noheda, J.A. Gonzalo, L.E. Cross, R. Guo, S.-E. Park, D.E. Cox, G. Shirane, Tetragonal-to-monoclinic phase transition in a ferroelectric perovskite: The structure of PbZr 0.52Ti0.48O3, Phys Rev B. 61 (2000) 8687–8695. https://doi.org/10.1103/PhysRevB.61.8687.

[58] J. Seidel, L.W. Martin, Q. He, Q. Zhan, Y.-H. Chu, A. Rother, M.E. Hawkridge, P. Maksymovych, P. Yu, M. Gajek, N. Balke, S. v Kalinin, S. Gemming, F. Wang, G. Catalan, J.F. Scott, N.A. Spaldin, J. Orenstein, R. Ramesh, Conduction at domain walls in oxide multiferroics, Nat Mater. 8 (2009) 229–234. https://doi.org/10.1038/nmat2373.

[59] T. Rojac, A. Bencan, G. Drazic, N. Sakamoto, H. Ursic, B. Jancar, G. Tavcar, M. Makarovic, J. Walker, B. Malic, D. Damjanovic, Domain-wall conduction in ferroelectric BiFeO3 controlled by accumulation of charged defects, Nat Mater. 16 (2017) 322–327. https://doi.org/10.1038/nmat4799.

[60] T. Sluka, A.K. Tagantsev, P. Bednyakov, N. Setter, Free-electron gas at charged domain walls in insulating BaTiO3, Nat Commun. 4 (2013) 1808. https://doi.org/10.1038/ncomms2839.

[61] J. Schaab, I.P. Krug, F. Nickel, D.M. Gottlob, H. Doğanay, A. Cano, M. Hentschel, Z. Yan, E. Bourret, C.M. Schneider, R. Ramesh, D. Meier, Imaging and characterization of conducting ferroelectric domain walls by photoemission electron microscopy, Appl Phys Lett. 104 (2014) 232904. https://doi.org/10.1063/1.4879260.

[62] L. Liu, T. Rojac, D. Damjanovic, M. di Michiel, J. Daniels, Frequency-dependent decoupling of domain-wall motion and lattice strain in bismuth ferrite, Nat Commun. 9 (2018). https://doi.org/10.1038/s41467-018-07363-y.

Ferroelectric Polycrystal

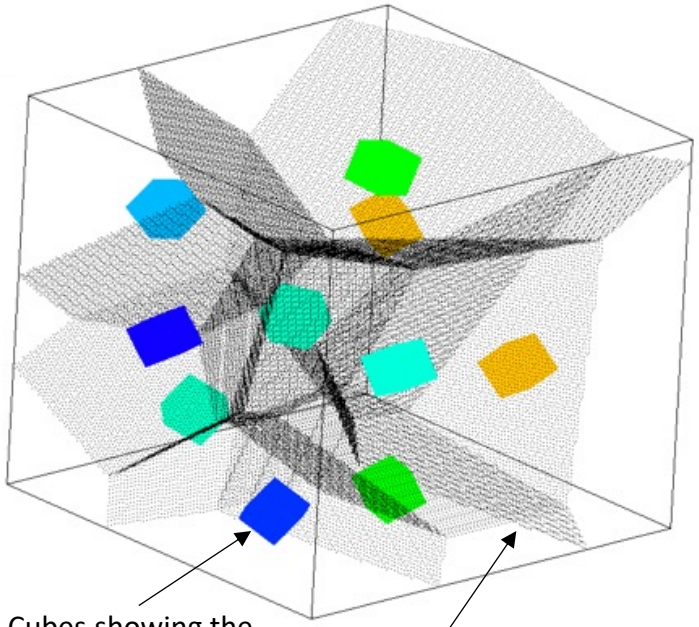

Cubes showing the crystallographic orientation of the grains

Dotted planes representing grain boundaries

Geometric Mismatch Minimization

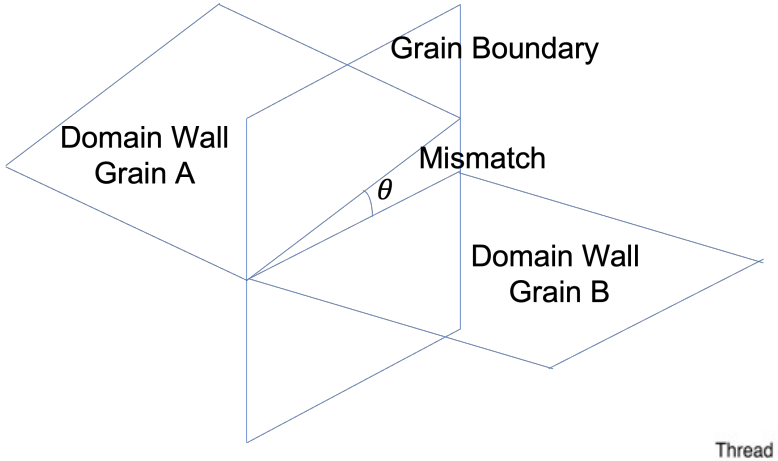

$$\text{Geometric Mismatch} = \cos^{-1}\{\hat{n}_{GB} \cdot (\hat{n}_{DW.grainA} \times \hat{n}_{DW,grainB})\}$$

Grain Boundary Residual Charge Minimization

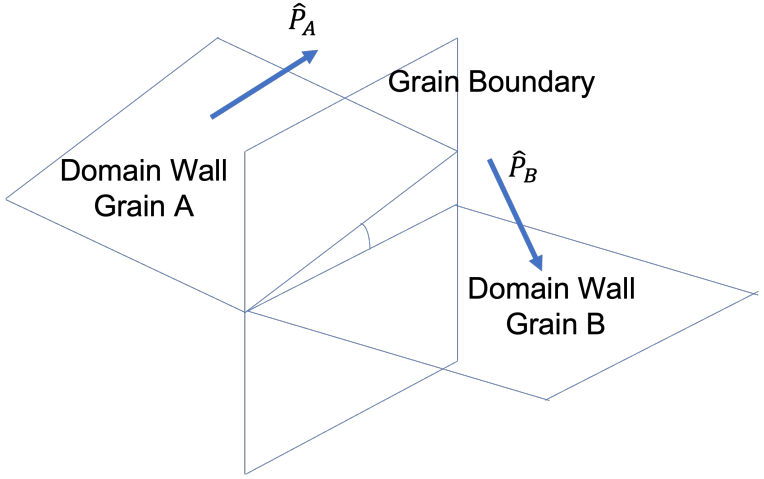

$$\text{Residual Charge} = \hat{P}_A.\hat{n}_{GB} - \hat{P}_B.\hat{n}_{GB}$$

Ferroelectric Domain Percolation